

**NASA TECHNICAL
MEMORANDUM**

Report No. 53937

**EFFECTS OF SPUTTERING PARAMETERS ON
TEFLON THIN FILM CAPACITORS**

By R. I. Miller
Clemson University

R. C. Ruff
Astronautics Laboratory

June 29, 1970

**CASE FILE
COPY**

NASA

*George C. Marshall Space Flight Center
Marshall Space Flight Center, Alabama*

1. REPORT NO. TM X-53937	2. GOVERNMENT ACCESSION NO.	3. RECIPIENT'S CATALOG NO.	
4. TITLE AND SUBTITLE Effects of Sputtering Parameters on Teflon Thin Film Capacitors		5. REPORT DATE June 29, 1970	
		6. PERFORMING ORGANIZATION CODE	
7. AUTHOR(S) R. I. Miller and R. C. Ruff		8. PERFORMING ORGANIZATION REPORT #	
9. PERFORMING ORGANIZATION NAME AND ADDRESS George C. Marshall Space Flight Center Marshall Space Flight Center, Alabama 35812		10. WORK UNIT NO.	
		11. CONTRACT OR GRANT NO.	
12. SPONSORING AGENCY NAME AND ADDRESS		13. TYPE OF REPORT & PERIOD COVERED Technical Memorandum	
		14. SPONSORING AGENCY CODE	
15. SUPPLEMENTARY NOTES Prepared by: Astronautics Laboratory Science and Engineering Directorate			
16. ABSTRACT The effects of varying the radio frequency (rf) sputtering parameters on the dielectric properties of resultant deposited thin films of Teflon is discussed. Electrode voltage, electrode spacing, and sputtering pressure were the parameters studied, and film thickness was the controlled variable. The dielectric constant, dissipation factor, dielectric strength, and resistivity were determined. In general, the dissipation factor increases with film thickness, while resistivity and dielectric strength decrease with increasing thickness. All parameters measured indicate a strong anomaly at 3 000 Å film thickness.			
17. KEY WORDS		18. DISTRIBUTION STATEMENT	
19. SECURITY CLASSIF. (of this report) Unclassified	20. SECURITY CLASSIF. (of this page) Unclassified	21. NO. OF PAGES 39	22. PRICE \$3.00

TABLE OF CONTENTS

	Page
SUMMARY	1
INTRODUCTION	1
DESCRIPTION OF APPARATUS	2
SAMPLE PREPARATION	6
EXPERIMENTAL PROCEDURE	6
DATA ANALYSIS	9
RESULTS	11
CONCLUSIONS	20
REFERENCES	31

LIST OF ILLUSTRATIONS

Figure	Title	Page
1.	Block diagram of sputtering system	3
2.	Radio frequency sputtering arrangement	5
3.	Masks for fabrication of three identical capacitors	7
4.	Circuit for measuring capacitance, dissipation factor, and current-voltage characteristics	8
5.	Breakdown test circuit	10
6.	Film thickness versus sputtering time	13
7.	Film thickness versus voltage	14
8.	Film thickness versus electrode spacing	15
9.	Dissipation factor versus time	16
10.	Dissipation factor versus voltage	17
11.	Dissipation factor versus electrode spacing	18
12.	Dissipation factor versus thickness	19
13.	Resistivity versus thickness	21
14.	Dielectric strength versus thickness	22
15.	Relative dielectric constant versus pressure	23
16.	Dielectric constant versus thickness	24

LIST OF TABLES

Table	Title	Page
1.	Parameters Varied During the Test Program	2
2.	Comparison of Bulk and Thin Film Teflon	12
3.	Teflon Films Composite Data Sheet for Series 1	25
4.	Teflon Films Composite Data Sheet for Series 2	25
5.	Teflon Films Composite Data Sheet for Series 3	26
6.	Teflon Films Composite Data Sheet for Series 4	27
7.	Teflon Films Composite Data Sheet for Series 5	28
8.	Teflon Films Composite Data Sheet for Series 6	29

EFFECTS OF SPUTTERING PARAMETERS ON TEFLON THIN FILM CAPACITORS

SUMMARY

It was expected that properties of sputtered Teflon thin films would differ from those of the bulk material. The sputtering parameters were varied in a controlled manner to determine the effect of these parameters on the properties of the sputtered thin film. Sputtering pressure (inert gas pressure), rf voltage, and electrode spacing were varied. Dielectric properties of the resulting thin film capacitors were then determined.

Film thickness was an almost linear function of sputtering time, as expected. Variation of sputtering voltage also produced a direct relationship, but lower voltage films were imperfect, and higher voltage films tended to be destroyed by intense heat build-up. Variation in electrode spacing was non-linear but indicated a trend toward less thickness with greater electrode spacing.

Dielectric parameters revealed some inconsistent behavior. The dissipation factor, however, will increase with film thickness, whereas resistivity and dielectric strength decrease with increasing film thickness. The dielectric constant varied with all parameters and could be optimized for each parameter. All dielectric properties revealed a strong anomaly, almost a discontinuity, at 3 000 Å.

INTRODUCTION

There has been interest in using thin Teflon films as insulators for printed microcircuits, printed circuit boards, and as the dielectric in capacitors for these circuits. Much information is available on the properties of bulk Teflon [1], but it was not previously known whether rf sputtered films would have these same properties. The work reported herein is an attempt to determine what properties of the thin films differ from bulk properties, and what sputtering parameters are responsible for this difference.

From the literature [2, 3], it was determined that four sputtering parameters should have more effect on film properties than any other. These are: time, inert gas pressure, rf voltage, and sputtering electrode spacing. During the course of the program, it was found that several more parameters could be added to this list, but these four are extremely important, and easy to manipulate and measure. The dielectric properties which were studied included dielectric constant, κ ; dissipation factor, D. F.; resistivity, ρ ; and breakdown voltage, $V_{B.D.}$, or the dielectric strength, $\vec{\nabla} V_{B.D.}$.

The program for studying the Teflon capacitor was arranged according to six series of samples listed in Table 1 along with the sputtering parameter which was varied in each series. The range of values for time and pressure was arbitrarily chosen except that the shortest time value was kept long enough to insure a measurable film thickness. Voltage values covered the entire range of useful voltages at fixed pressure and electrode spacing, while the electrode spacing was limited by the construction of the sputtering module.

TABLE 1. PARAMETERS VARIED DURING THE TEST PROGRAM

Series	Variable
1	time, at 110μ pressure of argon
2	time, at 80μ pressure of argon
3	time, at 60μ pressure of argon
4	rf voltage
5	sputtering electrode spacing
6	time, at 30μ pressure of argon

DESCRIPTION OF APPARATUS

A block diagram of the basic sputtering system is shown in Figure 1. The vacuum system is a glass bell jar with a mechanical pump. The pressure in the system is controlled by two mechanisms. A coarse adjustment is made

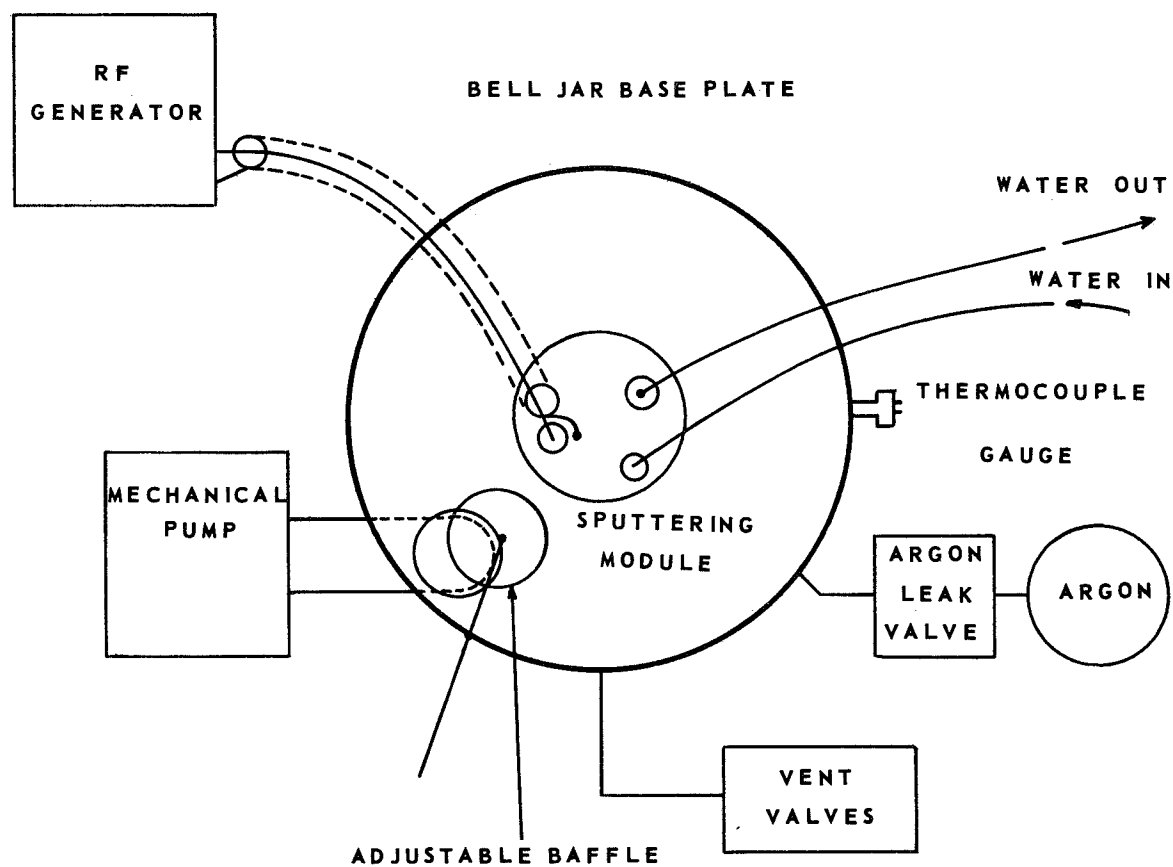


Figure 1. Block diagram of sputtering system.

with an adjustable baffle over the mechanical pump orifice. A fine adjustment is made by a micrometer valve in the argon gas input line. A vent valve is added for bringing the system to atmospheric pressure following a deposition. As mentioned earlier, the pressure for these depositions was controlled at various values between 30 and 110 microns as measured by a thermocouple pressure gauge in the bell jar.

The sputtering module itself was placed at the center of the bell jar base plate. Shown in the diagram are cooling water lines to the top of the module. These water hoses are made of a relatively strong vinyl material. Not shown in the diagram is a second set of hoses cooling the bottom of the module which is the substrate holder. The sputtering module will be more fully described later.

The last item in the sputtering system is the power supply. The radio frequency voltage from an rf generator was delivered to the sputtering module by a coaxial cable. Inside the vacuum chamber the coaxial cable was fabricated from heavy gage copper wire, Teflon tubing, and copper braid. The rf generator used was an existing 12 kW, 3.2 MHz power supply primarily used for induction heating. The power capabilities of this generator were not used. Instead the generator was operated with an internal induction load, and the voltage variation taken at the electrical center of the tank circuit was transferred to the sputtering module via the coaxial cable. The voltage measured and quoted in this report was the d.c. driving voltage used to power the oscillator tube.

A more detailed view of the sputtering module is shown in Figure 2. Shown is the Pyrex tube which is used both for containing the glow discharge and for supporting the top electrode assembly. The top electrode assembly consists of a grounded back shield or dark space shield, the Teflon source, and the metal electrode to which the rf voltage is applied. The bottom electrode consists of a grounded metal plate which supports the three glass substrates and a thin copper sheet used to mask the appropriate areas on the substrates from Teflon deposition. The inter-electrode spacing is variable and is controlled by raising or lowering the top Teflon support. As mentioned earlier, both the top and bottom electrode are water cooled to dissipate the heat generated by the glow discharge.

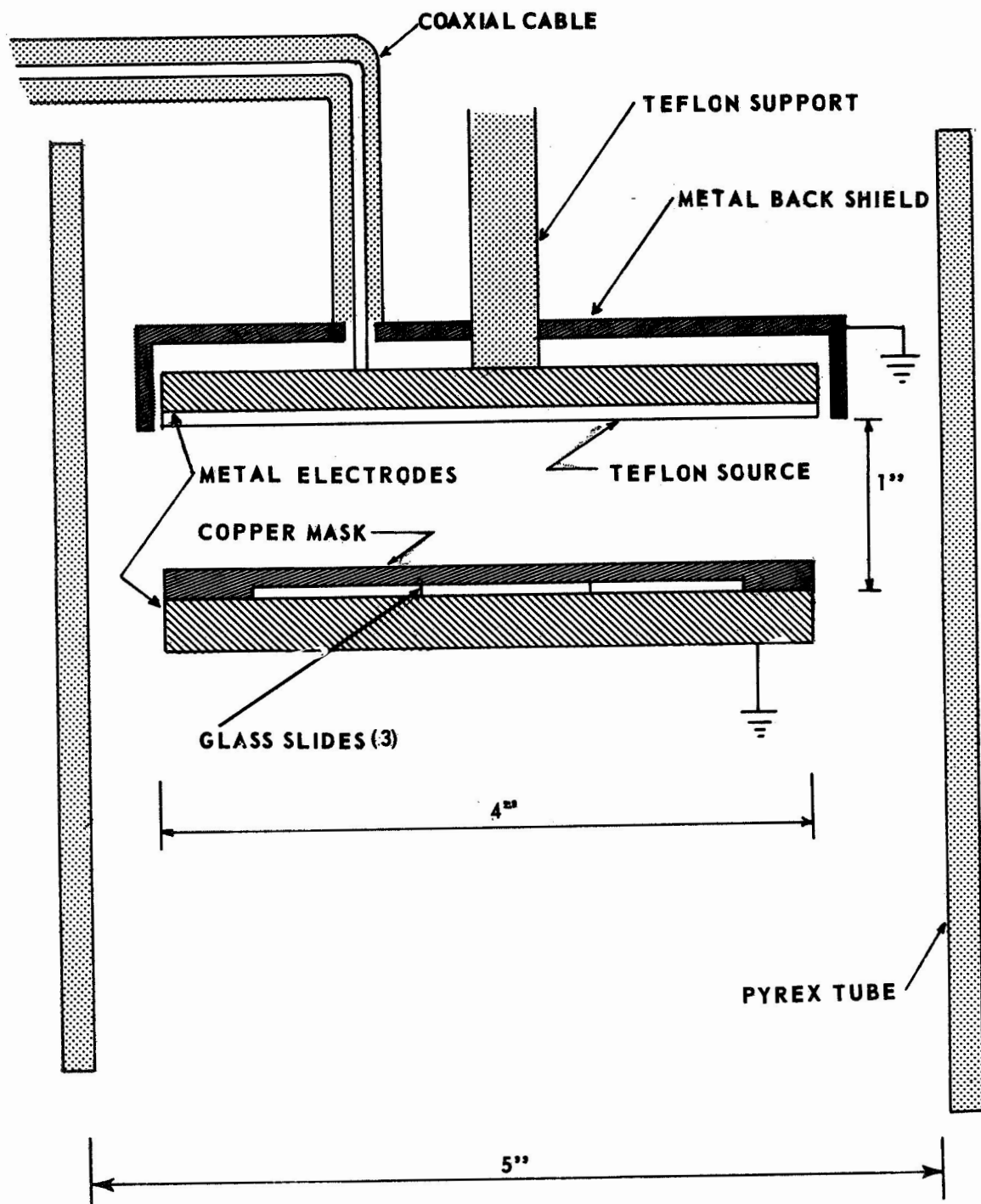


Figure 2. Radio frequency sputtering arrangement.

SAMPLE PREPARATION

The experimental capacitors were vacuum deposited on .025 by .076 meter (1 by 3 inches) glass microscope slides. These slides were cleaned by a 3-part wash-rinse cycle in an ultrasonic washer, followed by an alcohol rinse and air drying with a hot air blower. Since the capacitor's electrodes are aluminum thin films, it was impossible to solder leads to them; therefore a thick spot of conductive paint was placed at the two positions on the slide which would give best contact with the aluminum electrode while not affecting the shape of the capacitor. The paint was allowed to air-dry, then was baked at about 250° F.

The slide was then ready for deposition of the bottom electrode (Fig. 3). This was performed in a large vapor deposition vacuum system using a tungsten heater coil to evaporate the pure aluminum wire. Pressure for this deposition was nominally 10^{-6} torr.

After removing the slide from this system, it was placed in the sputtering system for deposition of the Teflon film. The sputtering electrode spacing would have been adjusted before closing the system. The rf voltage was set on the power supply, and the pressure in the system was regulated by both the argon input valve and a movable baffle located above the exit to the diffusion pump. When the voltage was applied, a glow discharge would begin and would continue, thus continuing film deposition until the voltage was removed after a specified amount of time.

The top electrode, which was deposited next, was made long enough to cover both ends of the rectangular Teflon film. This specification provided a reflecting surface at each end (one on top of the Teflon, one on top of bottom electrode) separated in height by exactly the height of the Teflon film. This reflecting surface made possible the measurement of film thickness with a source-imaging multiple-beam interferometer.

EXPERIMENTAL PROCEDURE

After soldering small copper wire leads to the paint terminals of the electrodes, a capacitor was ready to be tested. The capacitance and D. F. were measured first using an ordinary capacitance bridge, as indicated in Figure 4. Data were recorded at frequencies of 100 Hz, 1 kHz, and 10 kHz.

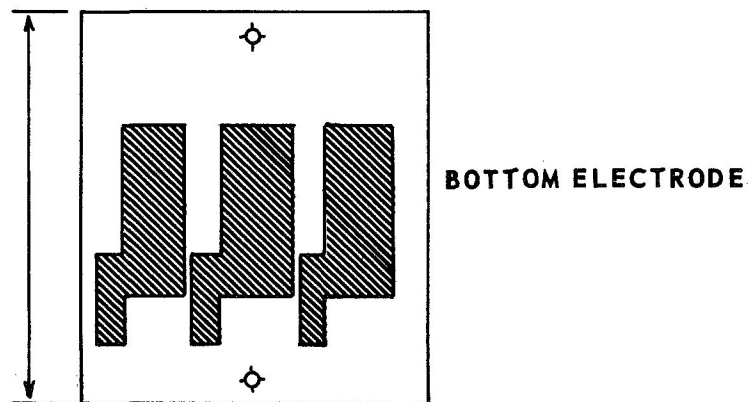
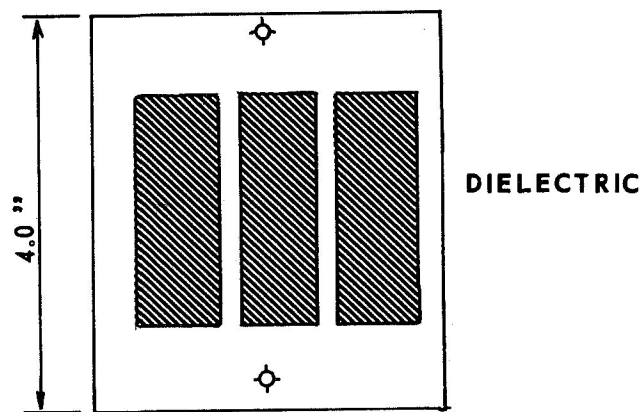
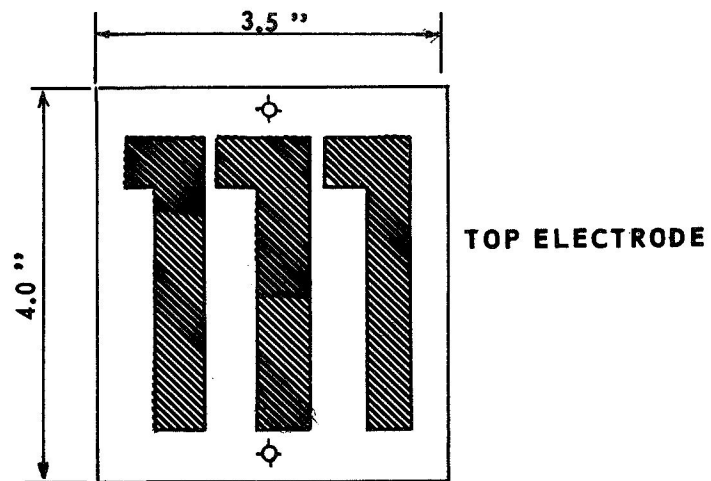


Figure 3. Masks for fabrication of three identical capacitors.
(Shaded area is cut out.)

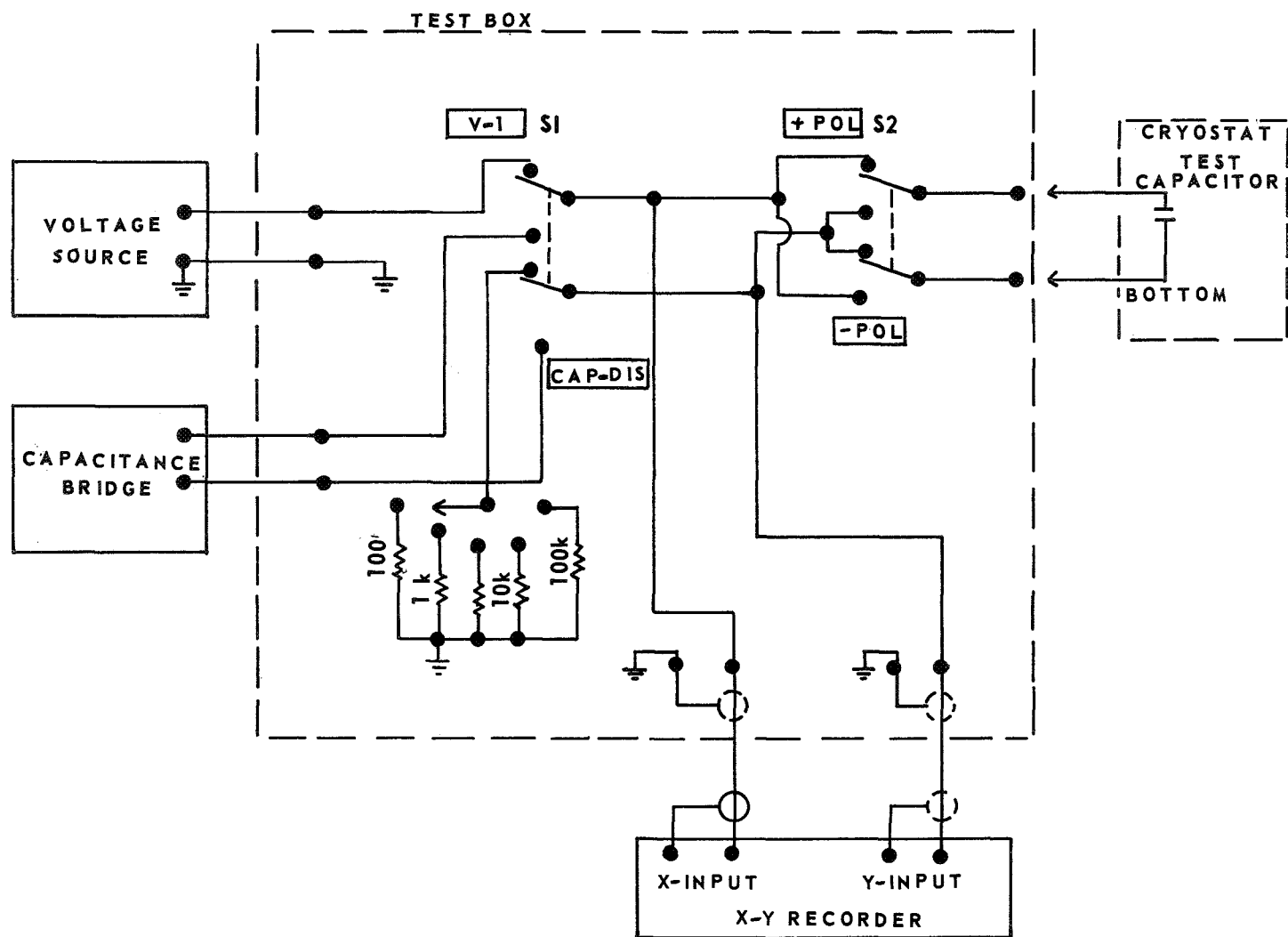


Figure 4. Circuit for measuring capacitance, dissipation factor, and current-voltage characteristics.

The circuit shown schematically in Figure 4 also was used to determine the current-voltage characteristic of the sample capacitor. The outputs were plotted on an X-Y recorder. Driving voltage was a low-frequency triangular waveform from a function generator.

Figure 5 [4] is a schematic of the breakdown voltage measuring circuit. The "ramp voltage" applied to the capacitors was the sawtooth output of the oscilloscope. This circuit was necessary to shunt the "ramp voltage" when the voltage reached values greater than the breakdown strength of the capacitor. At breakdown, the test capacitor discharge created a signal at the 0.05 uf capacitor which, after amplification, opened the gate of the SCR, thus shunting the voltage to the ground without passing through the Teflon in the test capacitor. The ramp voltage was displayed on a Tektronix 549 storage oscilloscope screen which stored the trace until the exact breakdown voltage had been measured from the screen grid. This process eliminated the need for taking photographs of each trace as it appeared.

DATA ANALYSIS

For bookkeeping purposes, each set of three slides was given a sample number, and each slide in the set was designated as 1, 2, or 3, depending on its position behind the deposition masks. For example, S180-3 was on the right side of all masks, while S180-1 was on the left. The thickness of each slide was measured at both ends and the average of these readings was the thickness recorded for the sample. It was noted that the thickness between one end of a capacitor and the other often varied by as much as a factor of 2, and the average thickness variation among the three slides was almost half as great.

The area (A) of the capacitor samples was 5.76 cm². From the equation for the capacitance of a parallel plate capacitor, the dielectric constant is given by:

$$\kappa = \frac{CT}{\epsilon_0 A} \quad (1)$$

where C is capacitance and T is Teflon film thickness [5].

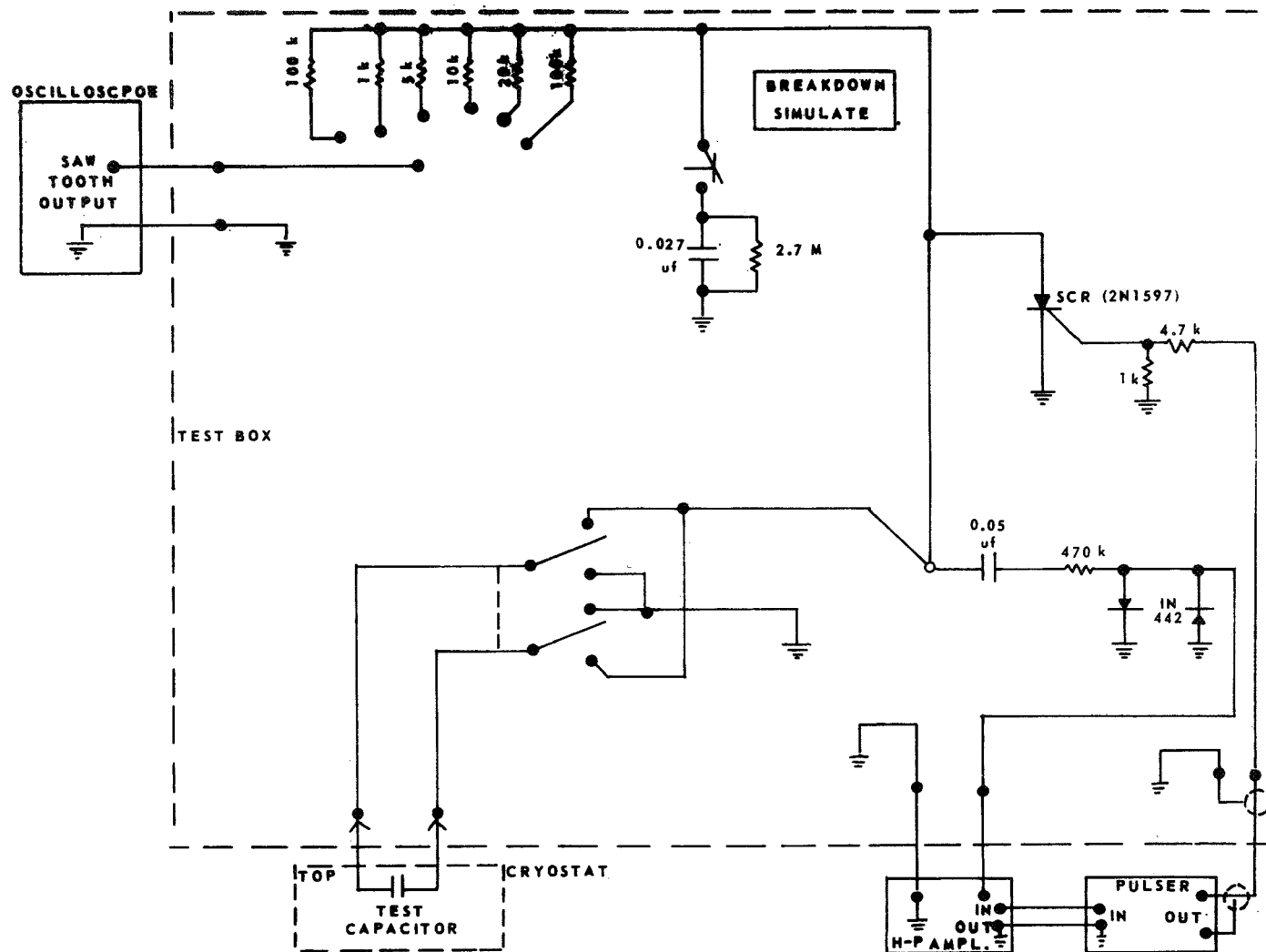


Figure 5. Breakdown test circuit.

The resistivity of thin film Teflon was calculated from [5]:

$$\rho = \frac{RA}{T} \quad (2)$$

where R, the ohmic resistance of the capacitor, was found from the current-voltage characteristic of the sample by:

$$R = \frac{\Delta I}{\Delta V} \quad (3)$$

The quantities on the right were calculated in the following manner. Voltage change, ΔV , is simply the product of the change in the X axis, with the recorder calibration factor F (in $\frac{\text{volts}}{\text{inch}}$):

$$\Delta V = (\Delta X) (F) \quad (4)$$

Current change, ΔI , is the corresponding product on the Y axis divided by the value of the monitoring resistor (10^3 ohms) whose voltage drop indicated the current. That is:

$$\Delta I = \frac{(\Delta Y) (F)}{10^3 \Omega} \quad (5)$$

Breakdown voltage was obtained by averaging the value of $V_{B.D.}$ over a series of eight ramps which comprised one sweep over the screen of the storage oscilloscope. The average value was rounded to the nearest volt.

RESULTS

In preparation for this study, three tests were conducted on Teflon films to learn something about their molecular structure. Samples of bulk and film Teflon were placed in a vacuum system and the outgassing analyzed as a function

of temperature with a mass spectrometer. The only result was that both types of Teflon were found to consist of the same basic monomer. When bulk and film samples were placed in a high vacuum, it was discovered that the thin film outgassed more and at lower temperatures than did the bulk sample. In an attempt to determine the type of bonding of Teflon molecules and their polarization (if any), an infra-red spectroscopic study was performed on three different films. Unfortunately all films were completely transparent to the ir radiation (too thin) and no information was obtained.

Film thickness was approximately a linear function of sputtering time (Fig. 6), as had been expected. There was much scatter in this data, and it is possible that at longer times, the time dependence becomes non-linear and increases more rapidly because of substrate heating effects. Also it can be seen that for a given interelectrode spacing and sputtering voltage, the gas pressure has no appreciable effect on sputtering rate from 60 to 100 μ . Figure 7 shows the voltage dependence of film thickness for the range 800 V to 1200 V. The samples prepared at 700 V had measurable thickness, but because each capacitor was shorted, no dielectric data were obtained. The samples prepared at 1300 V were destroyed by the intense heat which cracked the glass substrates or caused shorting of the aluminum electrode plates. In Figure 8, the variation in dielectric thickness with sputtering electrode separation is plotted. A non-linear decrease in thickness with increasing electrode separation is indicated, as would be expected.

The graphs of the dissipation factor as a function of time, voltage, and electrode spacing (Figs. 9-11) reveal no consistent behavior. However, Figure 12 indicates that D. F. will increase with film thickness, and that something causes a drastic change in D. F. in the neighborhood of 3000 Å. This "3000 Å anomaly" occurs in other data, as will be seen. It should also be noted (Table 2) that the D. F. for Teflon films is larger than the bulk Teflon value.

TABLE 2. COMPARISON OF BULK AND THIN FILM TEFLON

Property	Bulk Value [1]	Film Values
D. F.	2×10^{-4}	$5 \times 10^{-3} - 5 \times 10^{-2}$
ρ	$1.9 \times 10^{19} \Omega \text{ cm}$	$10^{13} - 10^{15} \Omega \text{ cm}$
$\vec{\nabla}V$ B. D.	$1.57 \times 10^5 \frac{\text{V}}{\text{cm}}$	$2 \times 10^5 - 5 \times 10^6 \frac{\text{V}}{\text{cm}}$
κ	2.1	1.4 - 7.4

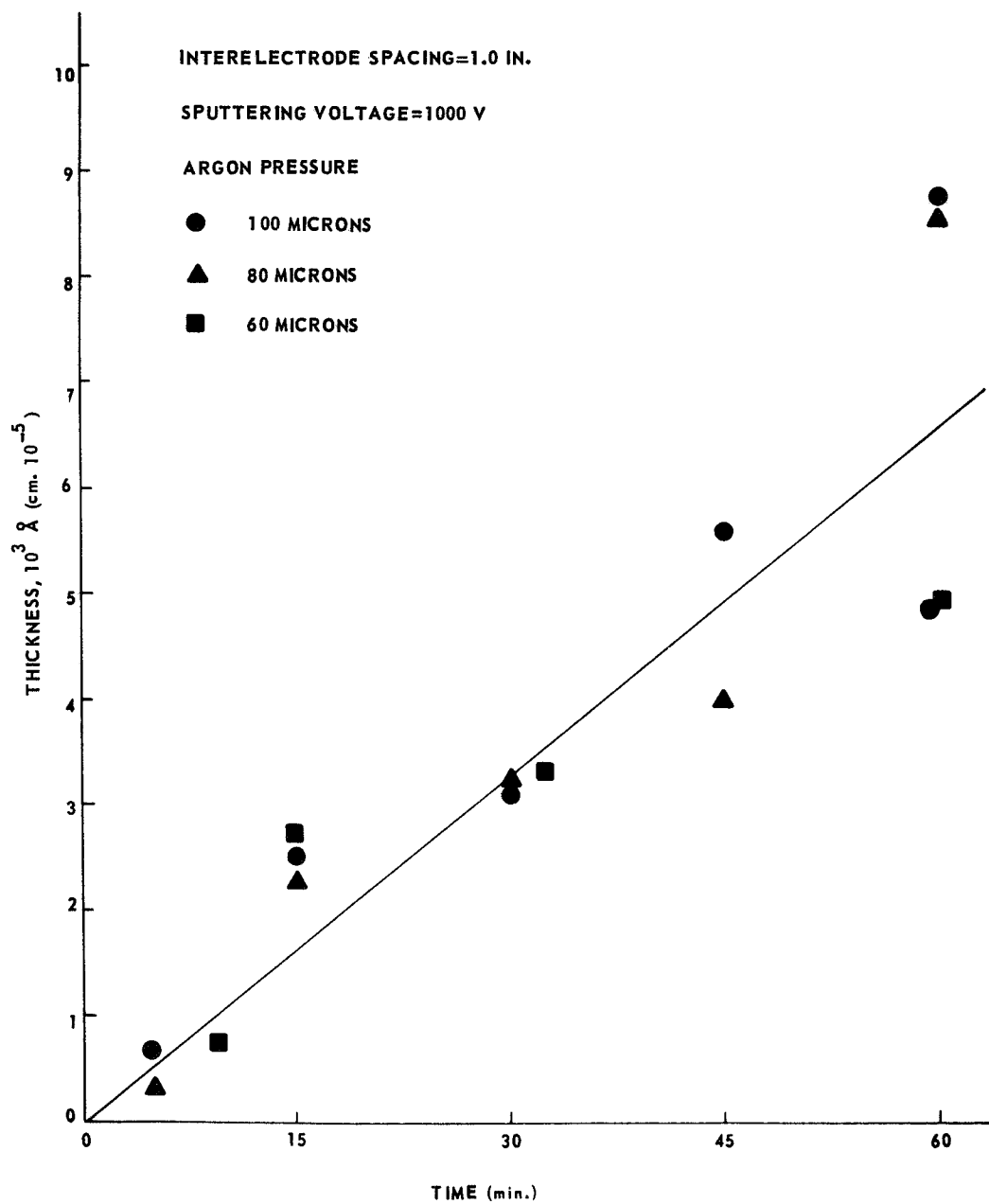


Figure 6. Film thickness versus sputtering time.

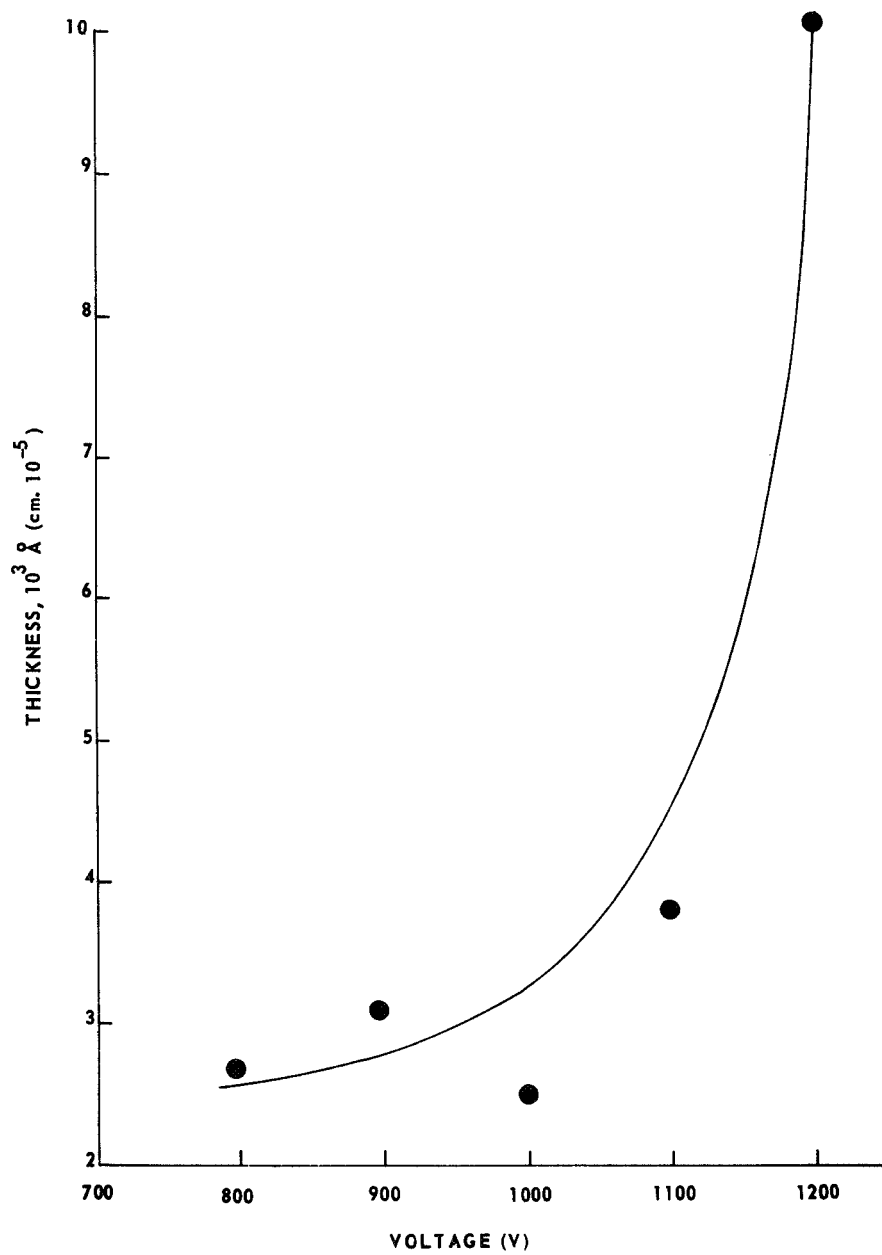


Figure 7. Film thickness versus voltage (series 4).

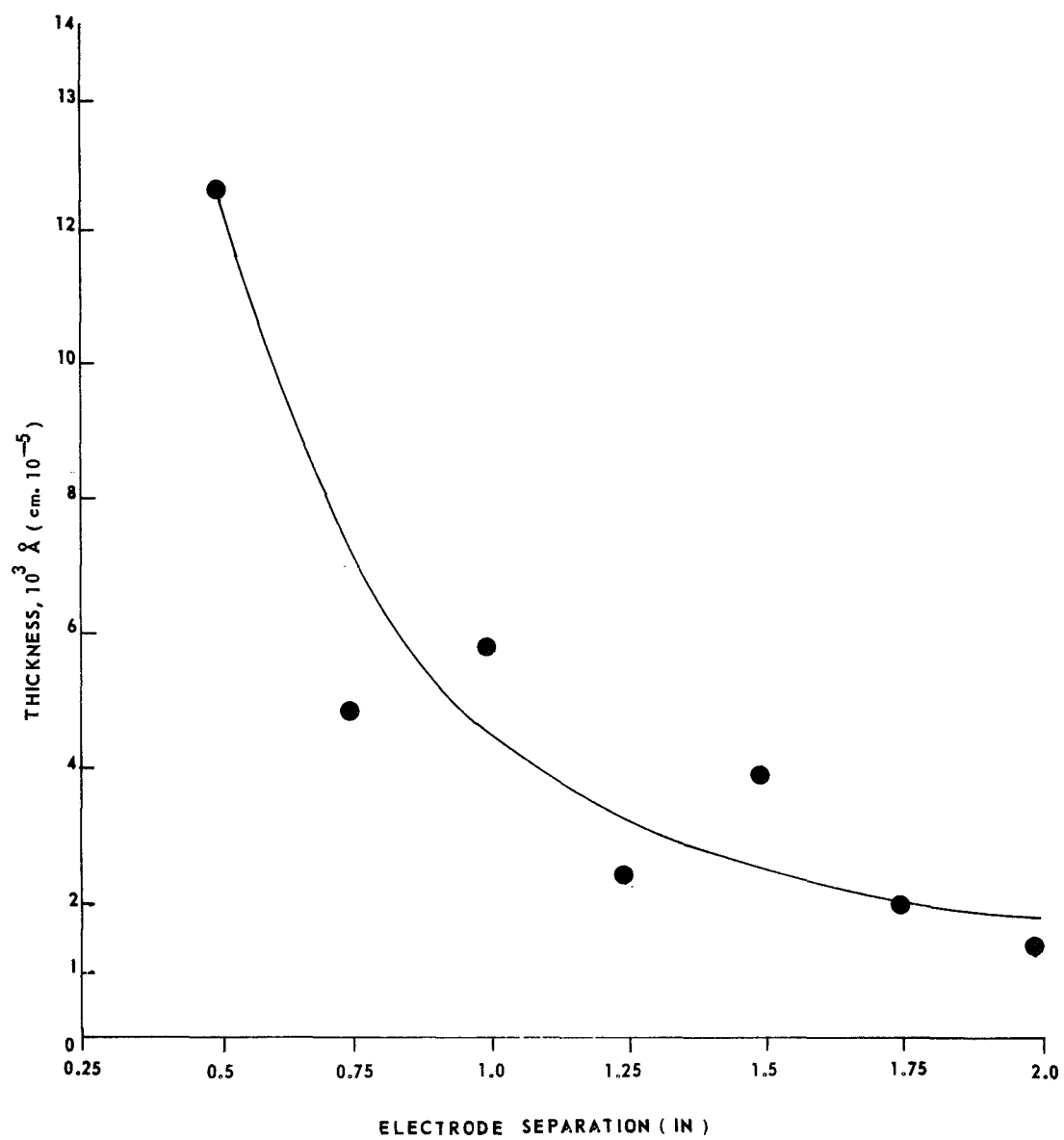


Figure 8. Film thickness versus electrode spacing.

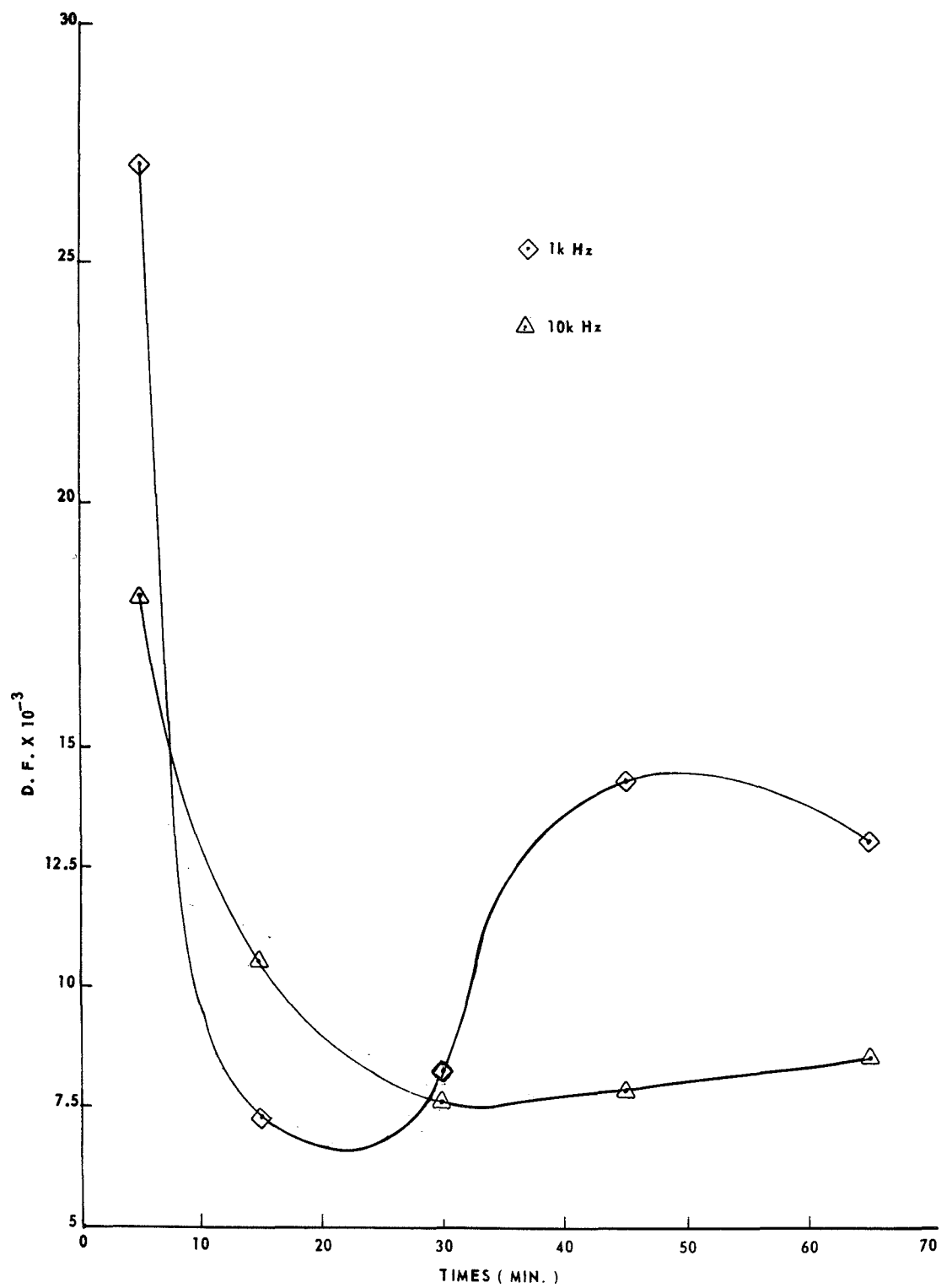


Figure 9. Dissipation factor versus time (series 1).

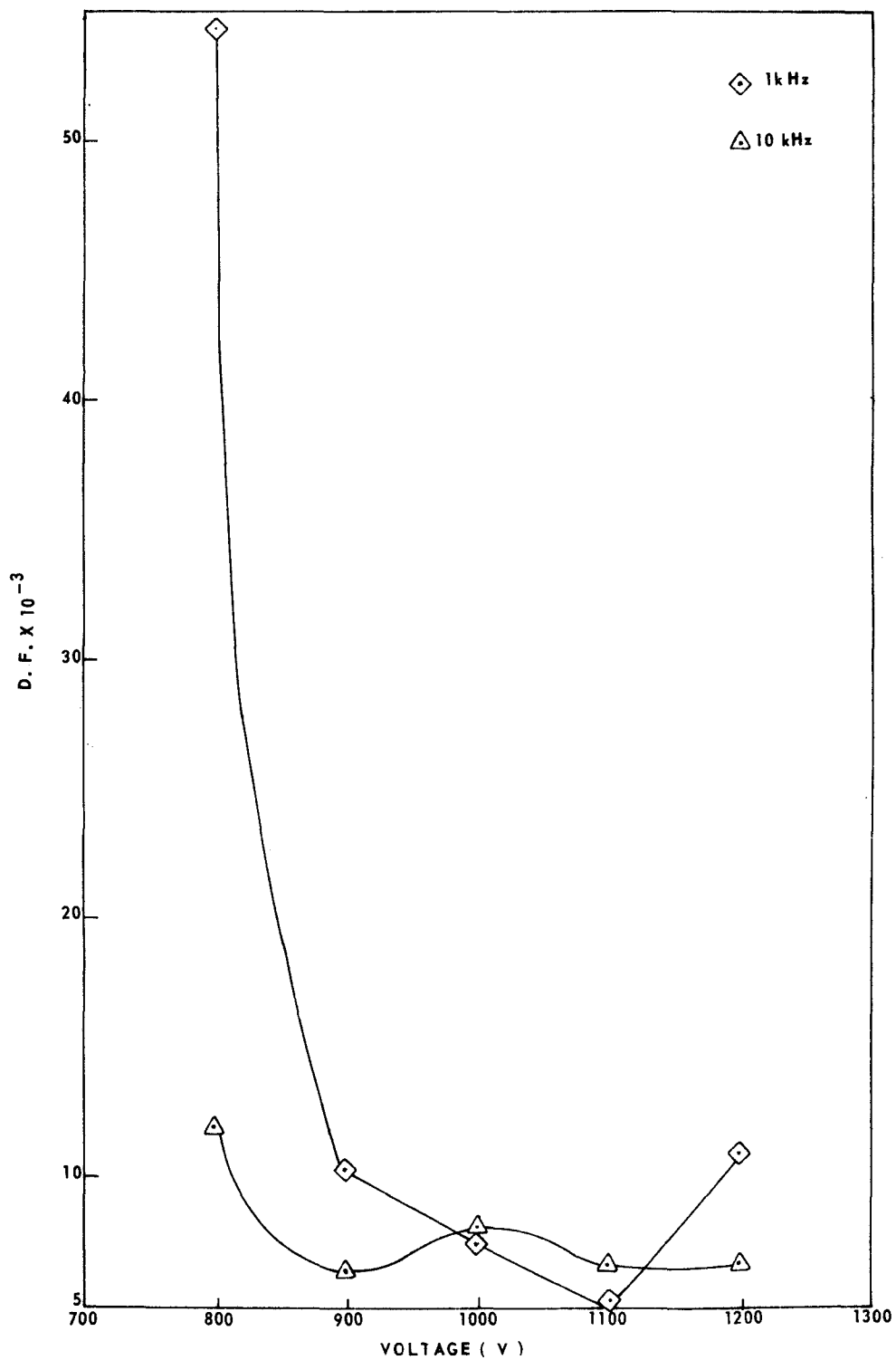


Figure 10. Dissipation factor versus voltage (series 4).

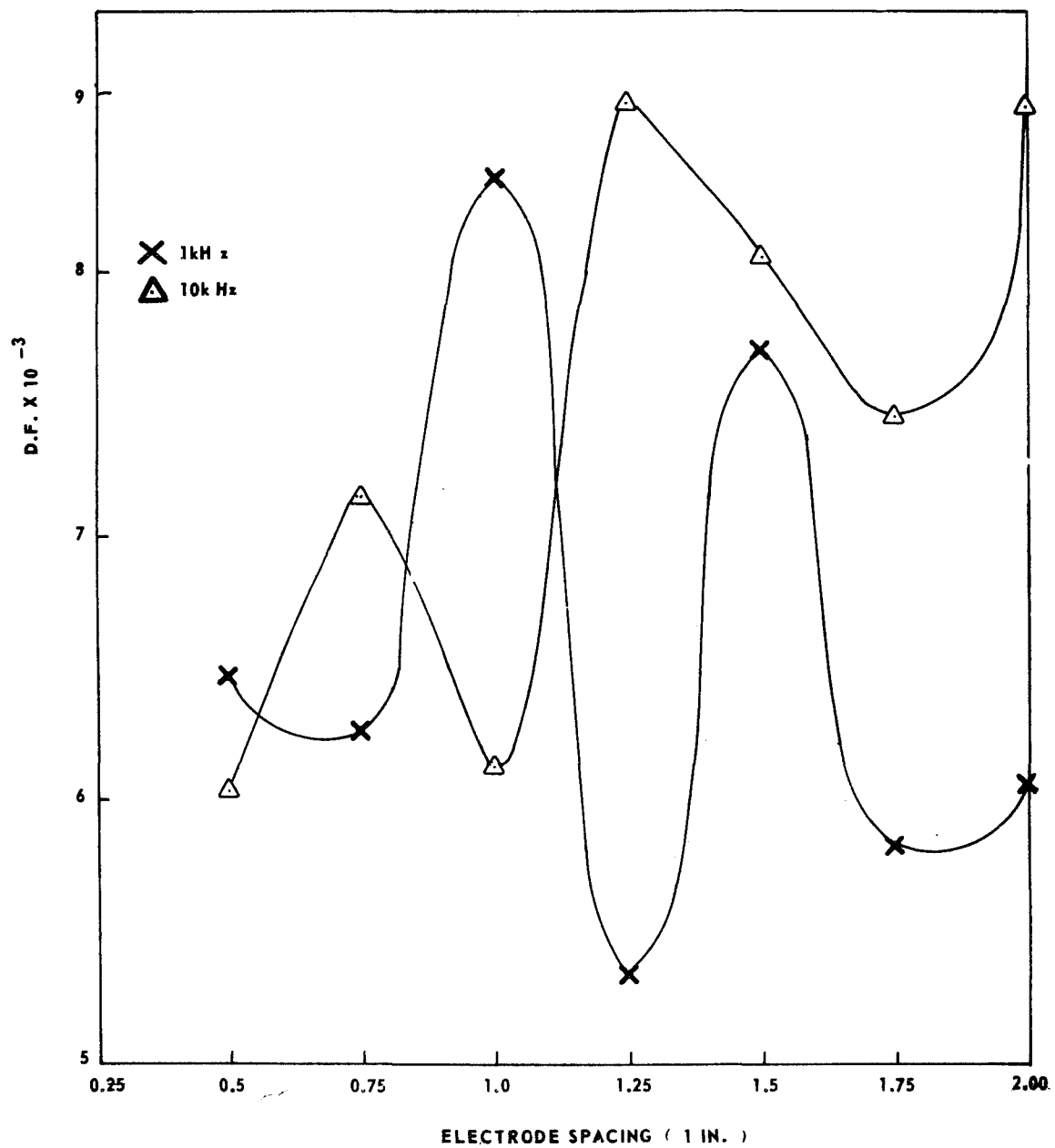


Figure 11. Dissipation factor versus electrode spacing (series 5).

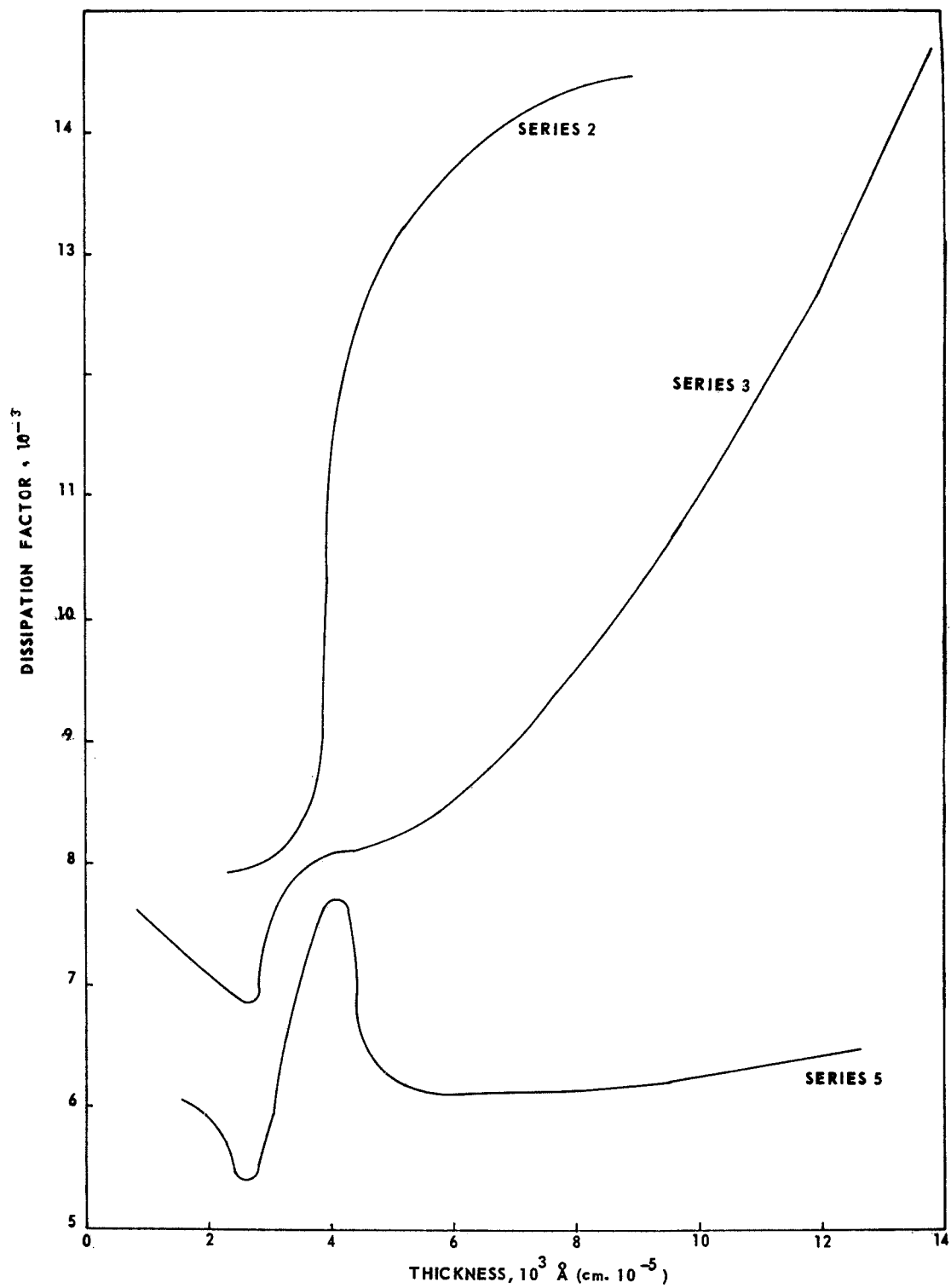


Figure 12. Dissipation factor versus thickness (at 1000 Hz)

Resistivity is shown (Fig. 13) only as a function of thickness, since it exhibits the same behavior for all series. Recall that in each series, a different combination of sputtering parameters was used to produce the different film thicknesses. In this graph, the anomaly occurs over the range of 3000 to 5000 Å, and at all times the resistivity is decreasing with increasing thickness. It was also found (Table 2) that the resistivity of the thin film Teflon was five orders of magnitude less than the bulk Teflon value.

Dielectric strength, or breakdown field (Fig. 14), is similar to resistivity in its dependence on thickness. This similarity is consistent in that a higher electric field is required to break down a relatively thin capacitor whose resistivity is higher than a thicker capacitor. These dielectric strength data agree in order of magnitude with the bulk Teflon dielectric strength [1]. It was observed that on all capacitors tested, breakdown occurred in the thin region of the Teflon film where the electric field has largest magnitude.

The graph of the dielectric constant, κ , as a function of sputtering pressure indicates that for given time, voltage, and electrode spacing a certain pressure will give the highest value for κ [Fig. 15]. The value of pressure at which this occurs is apparently dependent on the time of sputtering. A larger range of pressures should be studied to corroborate these statements.

The "3000 Å anomaly" is most obvious when the dielectric constant, κ , is plotted versus thickness [Fig. 16]. In this case the measured values of κ are very inconsistent near 3000 Å and do not fit smoothly into any curve through the remaining points. It is also seen that series 1, 2, and 3 have κ values near the bulk Teflon value, while series 4 and 5 (increasing voltage, decreasing electrode separation) increase almost linearly to much higher values at thicknesses greater than 6000 Å. In all cases, except series 2, κ increases monotonically with thickness above 6000 Å.

CONCLUSIONS

Several facts are clear from the figures presented and the inclusive data of Tables 3 through 8. Thickness of the Teflon films depends on sputtering time, rf voltage, and electrode separation, approximately as had been reported in the literature [2, 3], while argon gas pressure had no consistent effect on the thickness. The dissipation factor increases with film thickness for most series, and shows anomalous behavior near 3000 Å. Its value is always higher than the bulk Teflon D. F. value.

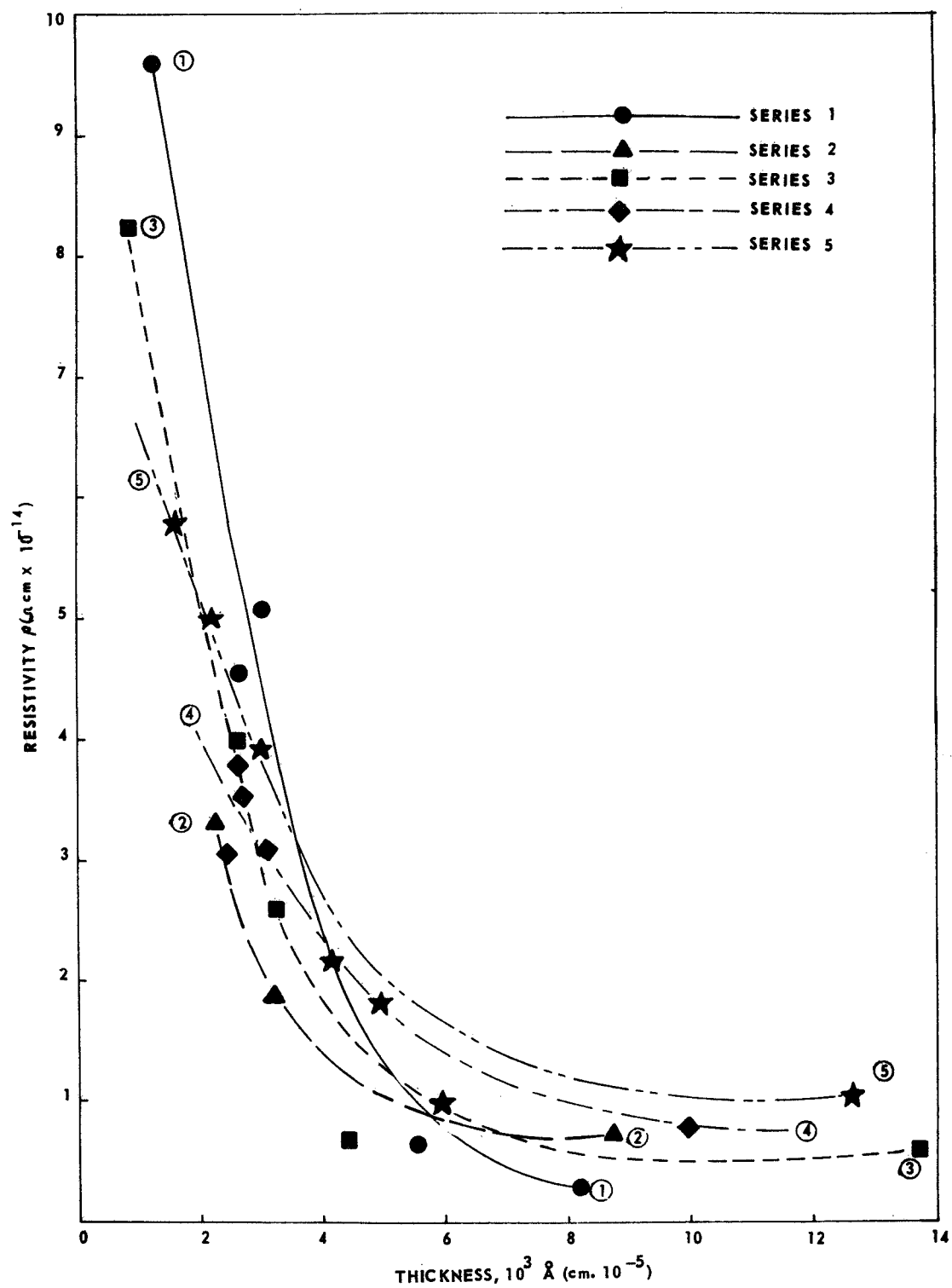


Figure 13. Resistivity versus thickness.

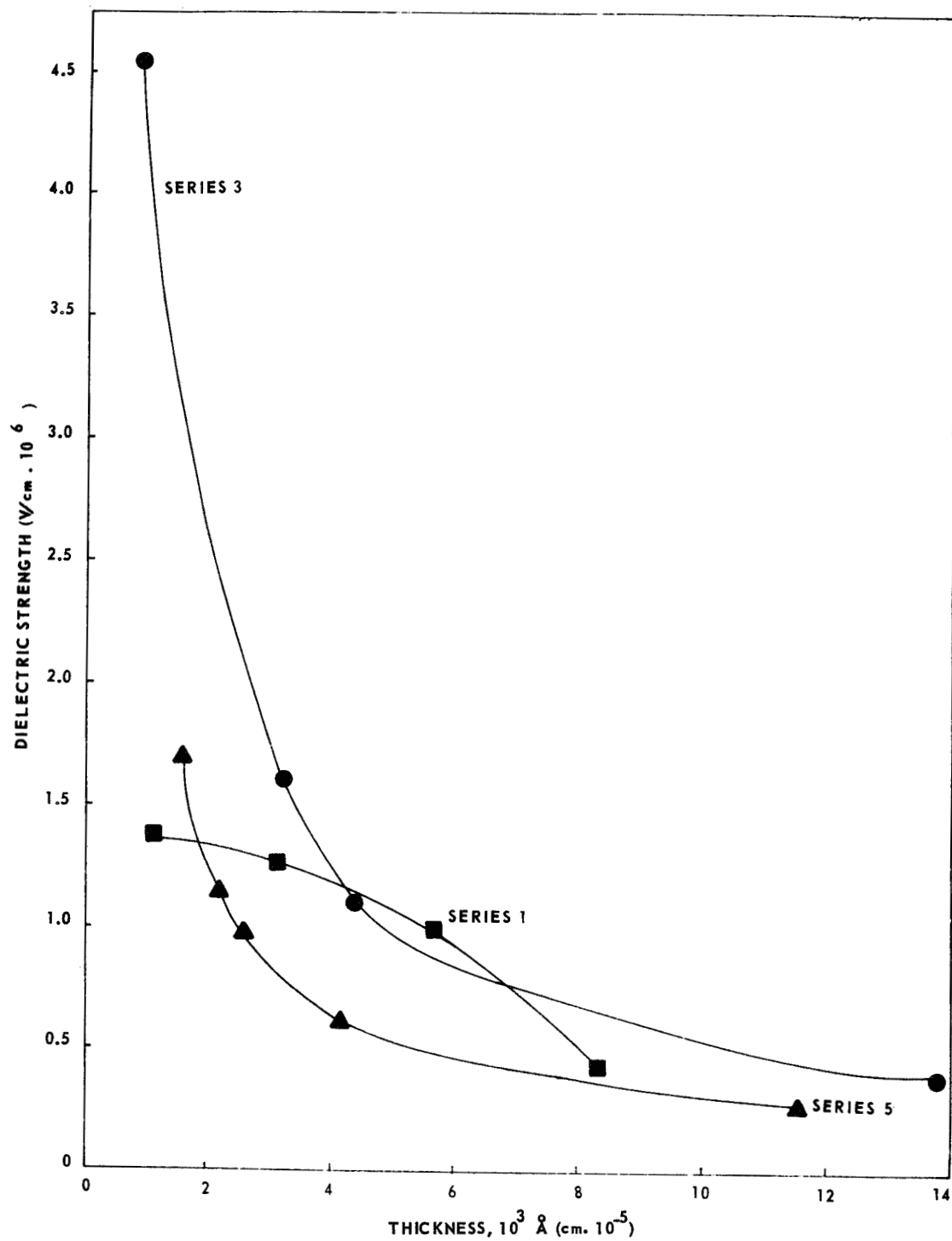


Figure 14. Dielectric strength versus thickness.

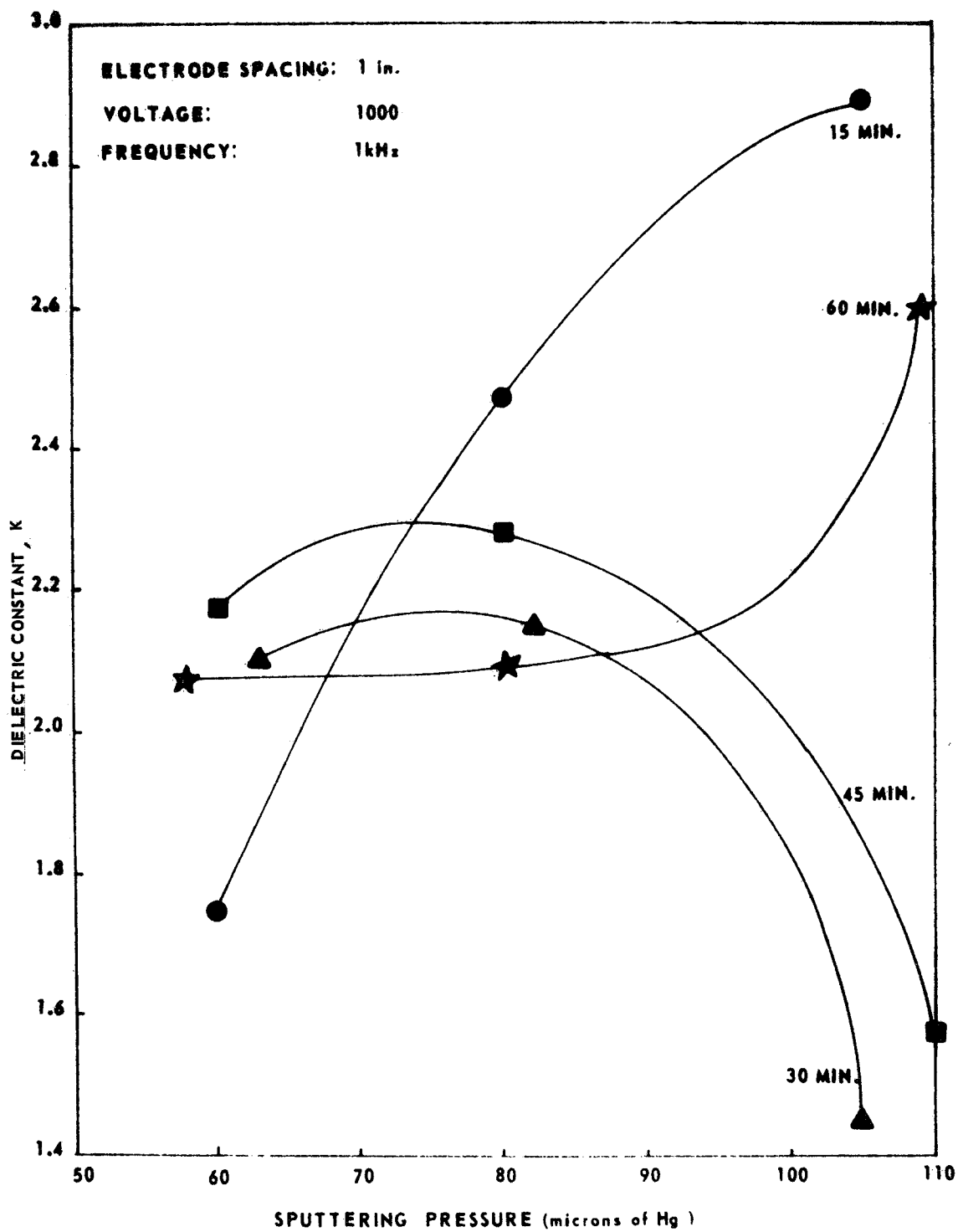


Figure 15. Relative dielectric constant versus pressure.

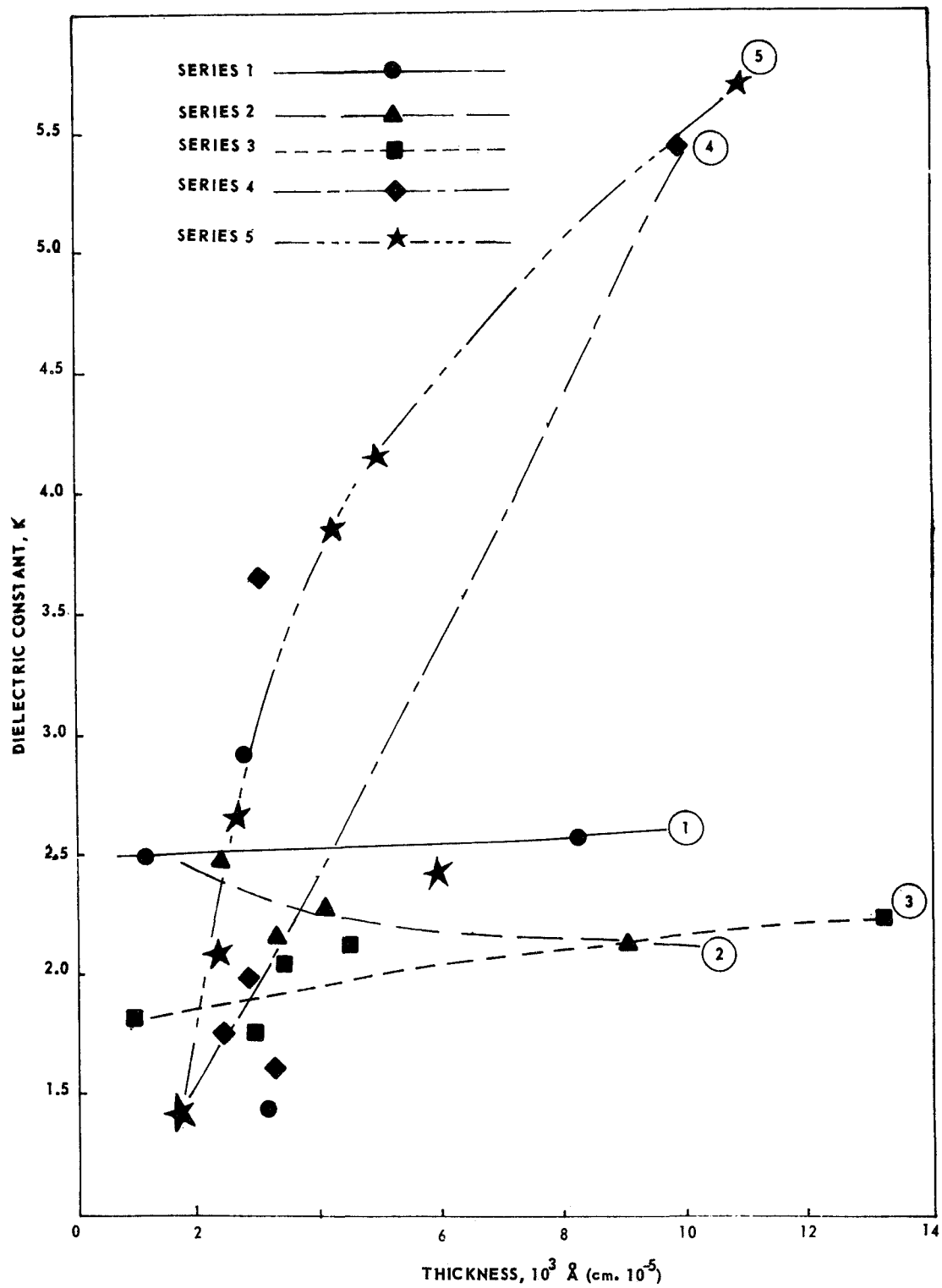


Figure 16. Dielectric constant versus thickness.

TABLE 3. TEFLON FILMS COMPOSITE DATA SHEET FOR SERIES 1

Sample Number	Electrode Spacing (in.)	Voltage (kV)	Pressure (μ)	Time (min)	Thickness \AA	Dep. Rate ($\text{\AA}/\text{min}$)	$\rho (\Omega \text{ cm})$ (10^{14})	V _{B. D.} (V)	F (kHz)	κ	D. F.	V _{B. D.} /T (V/cm)	Comments
S169-2	1	1	128	5	1 100	220	10.268	15	0.1 1.0 10.0	2.526 2.502 2.504	0.011 0.027 0.0181	1.36×10^5	$\nabla V_{B. D.}$ is $1.575 \times 10^5 \frac{V}{\text{cm}}$ [1].
S165-2	1	1	105	15	2 700	180	4.567	37	0.1 1.0 10.0	2.919 2.894 2.876	0.021 0.00725 0.0105	1.37×10^5	
S166-1	1	1	105	30	3 100	103	5.075	39	0.1 1.0 10.0	1.459 1.438 1.429	0.039 0.00825 0.0076	1.26×10^5	
S167-1	1	1	110	45	5 600	124	0.659	48	0.1 1.0 10.0	1.575 1.550 1.536	0.069 0.01424 0.00784	8.57×10^5 (0.98×10^6)	
S168-2	1	1	109	65	8 300	128	0.339	34	0.1 1.0 10.0	2.603 2.578 2.551	0.060 0.013 0.0085	4.10×10^5	V _{B. D.} from sample S167-2. B. D. on thin side of sample is 4909 \AA .

TABLE 4. TEFLON FILMS COMPOSITE DATA SHEET FOR SERIES 2

Sample Number	Electrode Spacing (in.)	Voltage (V)	Pressure (μ)	Time (min)	Thickness \AA	Dep. Rate ($\text{\AA}/\text{min}$)	$\rho (\Omega \text{ cm})$	V _{B. D.} (V)	F (kHz)	κ	D. F.	V _{B. D.} /T (V/cm)	Comments
S171-1	1	1000	80	15	2 300	153	3.333×10^{14}	31	0.1 1.0 10.0	2.499 2.470 2.450	0.028 0.00793 0.0099	1.35×10^6 (2.76×10^6)	B. D. on thin side of sample is 1 122 \AA .
S172-1	1	1000	82	30	3 200	107	1.891×10^{14}	None	0.1 1.0 10.0	2.171 2.149 2.134	0.028 0.0081 0.01007		
S173-1	1	1000	80	45	4 000	89	6.629×10^{10}	20	0.1 1.0 10.0	2.263 2.283 2.216	0.038 0.01112 0.01232	5×10^5	
S174-1	1	1000	80	60	8 900	148	0.761×10^{14}	32	0.1 1.0 10.0	2.1289 2.0874 2.0656	0.070 0.01444 0.00911	3.60×10^5	V _{B. D.} value after 980 ramps was 55. V _{B. D.} value given for S174-3.

TABLE 5. TEFLON FILMS COMPOSITE DATA SHEET FOR SERIES 3

Sample Number	Electrode Spacing (in.)	Voltage (V)	Pressure (μ)	Time (min)	Thickness (\AA)	Dep. Rate ($\text{\AA}/\text{min}$)	$\rho (\Omega \text{ cm}) (10^{14})$	$V_{B.D.}$ (V)	F (kHz)	κ	D. F.	$V_{B.D.}/T$ (V/cm)	Comments
S177-1	1	1000	60	10	840	84	8.233	38	0.1	1.828	0.010	4.52×10^6	B. D. on thin side: 692 \AA .
									1.0	1.803	0.0076	(5.49×10^6)	
									10.0	1.791	0.0210		
S176-1	1	1000	60	15	2 700	180	3.992	82	0.1	1.763	0.030	3.04×10^6	B. D. on thin side: 1726 \AA .
									1.0	1.754	0.00686	(4.75×10^6)	
									10.0	1.744	0.00777		
S175-1	1	1000	63	32	3 200	100	2.575	50.5	0.1	2.121	0.030	1.58×10^6	B. D. on thin side: 2577 \AA .
									1.0	2.107	0.00772	(1.96×10^6)	
									10.0	2.094	0.01100		
S178-1	1	1000	60	45	13 700	304	0.589	52	0.1	2.208	0.107	3.80×10^5	
									1.0	2.166	0.01468		
									10.0	2.152	0.00640		
S179-1	1	1000	58	60	4 400	73	0.689	48	0.1	2.096	0.040	1.09×10^6	
									1.0	2.075	0.0081		
									10.0	2.063	0.0742		

TABLE 6. TEFLON FILMS COMPOSITE DATA SHEET FOR SERIES 4

Sample Number	Electrode Spacing (in.)	Voltage (V)	Pressure (μ)	Time (min)	Thickness (\AA)	Dep. Rate ($\text{\AA}/\text{min}$)	$\rho (\Omega \cdot \text{cm})$	$V_{B.D.}$ (V)	F (kHz)	κ	D. F.	$V_{B.D.}/T$ (V/cm)	Comments
S183-2	1	800	80	30	2700	90	3.564×10^{10}	39.5	0.1 1.0 10.0	2.171 1.966 1.948	>0.1 0.0543 0.01194	1.46×10^6	B. D. on thin side of sample: 2 141 \AA .
S189-3	1	900	80	30	3100	103.3	3.160×10^{14}	63	0.1 1.0 10.0	1.631 1.614 1.605	0.066 0.0103 0.00645	2.03×10^6 (2.94×10^6)	
S172-3	1	1000	82	30	2500	83.3	3.066×10^{14}	None (shorted)	0.1 1.0 10.0	1.778 1.759 1.747	0.028 0.00753 0.00811		
S187-3	1	1100	80	30	2900	96.7	3.974×10^{11}	None (shorted)	0.1 1.0 10.0	29.500 28.756 28.488	0.027 0.01774 0.03923		
S184-2	1	1200	80	30	10 000	333.3	0.824×10^{14}	121	0.1 1.0 10.0	5.491 5.412 5.379	0.069 0.0110 0.00676	1.21×10^6	
S198-2	1 (Replaces S187-3)	1100	80	30	3800	123	1.742×10^{14}	26	0.1 1.0 10.0	3.658 3.638 3.626	0.02084 0.00519 0.00674	6.85×10^5	

TABLE 7. TEFLON FILMS COMPOSITE DATA SHEET FOR SERIES 5

Sample Number	Electrode Spacing (in.)	Voltage (V)	Pressure (μ)	Time (min)	Thickness (\AA)	Dep. Rate ($\text{\AA}/\text{min}$)	ρ ($\Omega \text{ cm}$) (10^{14})	$V_{\text{B. D.}}$	F (kHz)	κ	D. F.	$V_{\text{B. D.}}/T$ (V/cm)
S190-2	0.5	1000	80	30	12 600	420	1.0565	33	0.1 1.0 10.0	7.4777 7.4281 7.3918	0.03081 0.00648 0.00604	0.262×10^6
S191-1	0.75	1000	80	30	4900	163.3	1.8112	33	0.1 1.0 10.0	4.1295 4.1013 4.0787	0.02354 0.00627 0.00715	0.673×10^6
S192-3	1.0	1000	80	30	5900	196.7	0.9678	None (shorted)	0.1 1.0 10.0	2.4320 2.4106 2.3963	0.04462 0.00836 0.00613	
S193-1	1.25	1000	80	30	2600	86.7	3.8013	25	0.1 1.0 10.0	2.6380 2.6232 2.6127	0.0196 0.00535 0.00865	0.961×10^6
S194-2	1.50	1000	80	40	4100	102.5	2.1646	25.5	0.1 1.0 10.0	3.8599 3.8287 3.8089	0.03933 0.00771 0.00806	0.62×10^6
S195-1	1.75	1000	80	30	2200	73.3	4.9865	25	0.1 1.0 10.0	2.0533 2.0408 2.0305	0.02126 0.00583 0.00746	1.14×10^6
S196-1	2.00	1000	80	30	1600	53.3	5.7630	27	0.1 1.0 10.0	1.4112 1.4023 1.3950	0.02245 0.00607 0.00864	1.69×10^6

TABLE 8. TEFLON FILMS COMPOSITE DATA SHEET FOR SERIES 6

Sample Number	Electrode Spacing (in.)	Voltage (V)	Pressure (μ)	Time (min)	Thickness (\AA)	Dep. Rate ($\text{\AA}/\text{min}$)	$\rho (\Omega \text{ cm})$ (10^{14})	$V_{\text{B. D.}}$	F (kHz)	κ	D. F.	$V_{\text{B. D.}}/T$ (V/cm)
S181-2	1	1000	30	45	440	9.8	0.303	87	0.1	1.150	0.041	2×10^7
									1.0	1.099	0.024	
									10.0	1.071	0.02382	
S199-1	1	1000	25	60	6800	113.3	0.795	34	0.1	2.828	0.08179	5.0×10^5
									1.0	2.788	0.01274	
									10.0	2.770	0.01447	
S200-3	1	1000	30	75	8200	109.3	1.427	113	0.1	2.718	0.08781	1.38×10^6
									1.0	2.686	0.01404	
									10.0	2.669	0.00662	

Resistivity of Teflon films was approximately $10^5 \Omega\text{cm}$ less than bulk Teflon resistivity, and exhibits the "3000 Å anomaly." Resistivity was found to increase with decreasing film thickness. Dielectric strength also increased with decreasing thickness and exhibited values comparable to bulk Teflon over most of the thickness range.

The dielectric constant of Teflon films is within 36 percent of the bulk Teflon value for the series in which time and pressure were varied, but becomes 3 times larger (at higher thickness) for the series where rf voltage and sputtering electrode spacing were varied. The "3000 Å anomaly" is most obvious in these data; and for thicknesses above 6000 Å in series 4 and 5, the dielectric constant increases in an almost linear fashion with thickness.

It can now be seen that rf sputtered Teflon thin films differ from bulk Teflon in their dielectric properties, and that the differences are caused by parameters in the sputtering process. The dielectric constant is influenced by electrode spacing in the sputtering module, and by the rf voltage applied to the electrode. The dissipation factor is influenced by sputtering time, though it is not certain what causes it to differ from bulk Teflon by one to two orders of magnitude. The dielectric strength for the films was comparable to bulk Teflon in value and showed a thickness dependence similar to bulk samples. Resistivity of the films differed most drastically from bulk Teflon resistivity values. The difference is believed to be caused by impurities and the state of the Teflon molecules when deposited on the substrate in the sputtering chamber, though more work is required to verify this. Studying the dependence of resistivity on temperature and applying a d. c. bias voltage to the grounded sputtering electrode should give insight into this question.

Other items deserve further consideration, such as the "3000 Å anomaly" and the almost linear relation between κ and thickness for some samples which yields very large values of κ . The large variation in film thickness on a given sample is a practical problem yet to be solved. Bonding the Teflon disk to be sputtered to the metal electrode instead of bolting it (with Teflon bolts as was done in the present work), would eliminate non-uniform fields which may now exist on the sputtering face of the disk causing non-uniform sputtering rates and deposition.

REFERENCES

1. Gillespie, et al.: New Design Data for Teflon Fluorocarbon Resins. Machine Design; Part 1, January 21, 1960; Part 2, February 18, 1960.
2. Holland, L.: Vac-Deposition of Thin Films. Chapman and Hall (London), 1963.
3. Blevis, E. H.; and Holritz, C. A.: R-F Glow Discharge Sputtering. R. D. Mathis Co., 1965.
4. Hayes, P. J.: Breakdown in Vacuum Deposited Thin Film Silicon Monoxide Capacitors. Supplement to Final Report, NAS 8-11279.
5. Duckworth, H. E.: Electricity and Magnetism. Holt, Rinehart, and Winston (New York), 1961, Chs. 3 and 5.

EFFECTS OF SPUTTERING PARAMETERS ON TEFLON THIN FILM CAPACITORS

By R. I. Miller and R. C. Ruff

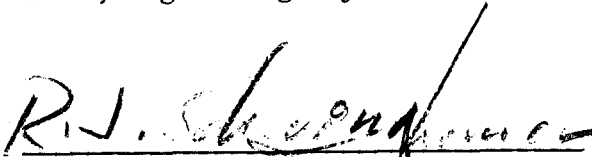
The information in this report has been reviewed for security classification. Review of any information concerning Department of Defense or Atomic Energy Commission programs has been made by the MSFC Security Classification Officer. This report, in its entirety, has been determined to be unclassified.

This document has also been reviewed and approved for technical accuracy.



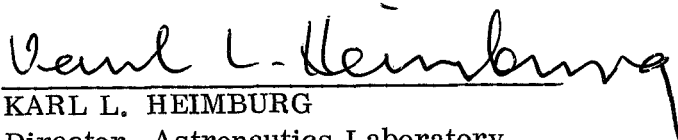
R. L. GAUSE

Chief, Engineering Physics Branch



R. J. SCHWINGHAMER

Chief, Materials Division



KARL L. HEIMBURG

Director, Astronautics Laboratory

DISTRIBUTION

TM X-53937

DIR DEP-T	S&E-ASTN-MM Mr. McKannan
AD-S Dr. Stuhlinger	S&E-ASTN-MC Mr. Nunnelley
PM-PR -M Mr. Goldston	S&E-ASTN-MN Mr. Curry
S&E-CSE-DIR Dr. Haeussermann	S&E-ASTN-ME Dr. Gause
S&E-ASTN-DIR Mr. Heimburg Mr. Kingsbury	S&E-ASTN-RM Miss Scott
S&E-ASTN-E Mr. Kroll	S&E-ASTN-MEV Mr. Horton Mr. Ruff (25)
S&E-ASTN-P Mr. Paul	S&E-SSL-DIR Mr. Heller
S&E-ASTN-T Mr. Grafton	S&E-SSL-P Mr. Hembree Dr. Dozier
S&E-ASTN-S Mr. Isbell	S&E-SSL-PO Mr. Moore
S&E-ASTN-A Mr. Sterett	S&E-ASTR-DIR Mr. Moore
S&E-ASTN-M Mr. Schwinghamer (6) Mr. Holmes Mr. Riehl Mr. Uptagrafft	S&E-ASTR-RP Mr. Griner
	A&TS-MS-IP Mr. Remer

DISTRIBUTION (Concluded)

TM X-53937

A&TS-MS-IL

Miss Robertson (8)

A&TS-TU

Mr. Wiggins (6)

A&TS-MS-H

Mr. Akens

A&TS-PAT

Mr. Wofford

PM-PR-M

Scientific and Technical Information

Facility (25)

P. O. Box 33

College Park, Maryland 20740

Attn: NASA Representative (S-AK/RKT)